

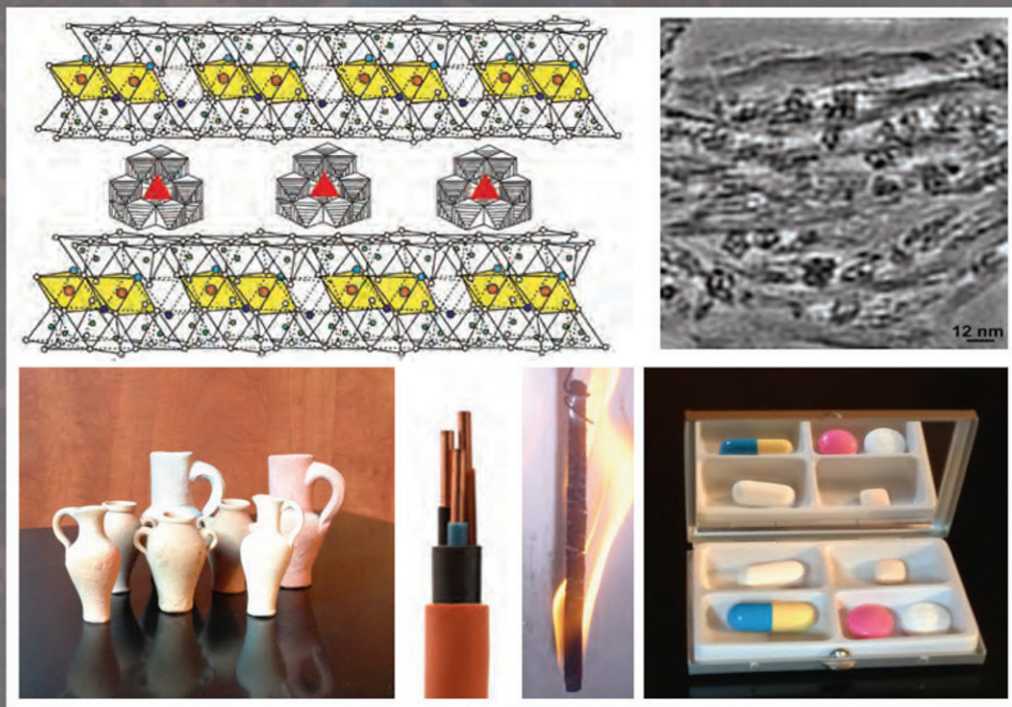
HANDBOOK OF CLAY SCIENCE

SECOND EDITION

PART B: TECHNIQUES AND APPLICATIONS

EDITED BY

F. BERGAYA AND G. LAGALY



Molecular Simulation of Clay Minerals

J.A. Greathouse and R.T. Cygan

Geochemistry Department, Sandia National Laboratories, Albuquerque, New Mexico, USA

Chapter Outline

3.1. Introduction	405	3.4.2. Interlayer Structure and Dynamics	411
3.2. Simulation Basics	407	3.4.3. Solute Adsorption	414
3.3. Force Field Development	409	3.5. Concluding Remarks	419
3.4. Applications	410	References	420
3.4.1. Clay Mineral Swelling	410		

3.1 INTRODUCTION

Molecular simulation involves the use of computational chemistry methods to provide an atomistic description of chemical or physical processes (i) for interpretation of experimental results and (ii) to shed light on the molecular structure of a chemical system for which experimental data are difficult to obtain or interpret. These methods can also be used as a predictive tool to be later verified with new experiments. They are particularly relevant to the study of clay minerals, whose small particle size and complex chemistry make them unsuitable for structural analysis such as single-crystal X-ray diffraction.

Although molecular simulation spans several levels of theory, from highly accurate quantum mechanics to the mesoscale level, here we focus on classical methods in the form of molecular dynamics (MD) or Monte Carlo (MC) simulation. These classical simulation methods use approximate energy expressions to describe the interaction between atoms and molecules. In both methods, the total potential energy of the system is calculated from pairwise or multi-body interaction potentials (see Section 3.2). In MD simulation, the equations of motion are simultaneously solved for every particle in the model system. The time evolution of the model system is then analyzed to calculate the desired properties. In MC simulation, the system evolves through random moves which

are accepted or rejected according to a Boltzmann algorithm. The equilibrium configuration space of a system is sampled during the production portion of the simulation, yielding a wealth of structural and thermodynamic properties. For more detail, the reader is referred to a thorough introduction of modelling methods applied to geochemistry (Cygan, 2001), and a well-known monograph on molecular simulation (Frenkel and Smit, 2002).

The results of these classical methods are only as reliable as the parameters used in the simulations, but the accessible length scales (hundreds of nanometres) and time scales (hundreds of nanoseconds) justify the use of approximate methods. For example, simulations involving an interface between an aqueous solution and a clay mineral surface are well within the ability of classical simulations but still beyond reach of the more accurate quantum methods. A sampling of typical experimental clay mineral properties is given in Table 3.1 with their analogous simulation properties.

The first papers on molecular simulations of clay minerals were published 20 years ago (Delville, 1991; Skipper et al., 1991). These early articles were limited in accessible length and time scales due primarily to limitations in computer resources. However, the rapid improvement in computer technology, especially the growth of multi-processor computers and processor speed, led to a steady increase in the use of simulation methods to study clay minerals. Thus, the number of publications in this area continues to grow (Fig. 3.1).

TABLE 3.1 Methods of Obtaining Clay Mineral Observables from Experiment or Simulation

Property	Experiment	Simulation
Unit cell parameters	Diffraction	Energy minimization, constant-pressure simulation
Local atomic coordination	EXAFS, structure factor	Radial distribution function
Interfacial structure	X-ray scattering	Atomic density profiles
Contact angle	Microscopy, microtomography	MD simulation
Mechanical properties	Nanoindentation	Energy minimization, MC or MD simulation
Diffusion	NMR, neutron scattering	Mean square displacement (MD simulation)
Vibrational motion	Spectroscopy (IR, Raman)	Normal mode analysis, power spectra (MD simulation)

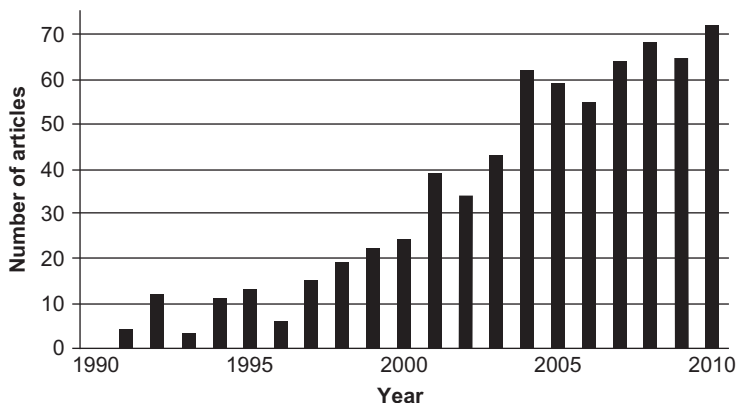


FIGURE 3.1 Literature search for published articles using *Web of Science*SM for keywords (clay + ‘molecular dynamics’) or (clay + ‘Monte Carlo’).

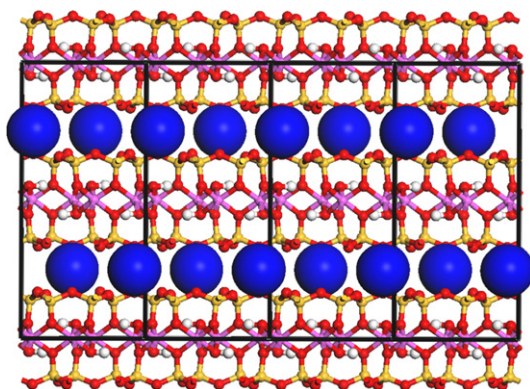


FIGURE 3.2 Several unit cells (black lines) of non-hydrated Na⁺-montmorillonite (Na⁺-Mt) demonstrating the use of periodic boundary conditions in molecular simulations.

3.2 SIMULATION BASICS

Molecular simulations utilize periodic boundary conditions in which a finite-sized model system is repeated infinitely in three dimensions to effectively represent a macroscopic physical system. With well-defined unit cells, minerals and mineral interfaces are ideally suited for simulation using periodic boundary conditions. This concept is demonstrated in Fig. 3.2 with Na⁺-Mt. Movement of an atom in the primary cell causes its periodic image to be moved by the same amount in every other cell.

The underlying theory behind both MC and MD simulation comes from statistical mechanics in which thermodynamic ensembles are used to describe the equilibrium properties of a system. Examples of ensembles include

microcanonical (NVE), canonical (NVT), isothermal-isobaric (NPT), and grand canonical (μVT), where N is the number of particles in the model system, V is the volume, E is the total potential energy, T is the temperature, P is the pressure, and μ is the chemical potential. Likewise, molecular simulations are performed under the constraint of such an ensemble. Constant-temperature and constant-pressure simulations require a thermostat or a barostat, respectively, to maintain the system at the desired temperature or pressure. Ensemble averages are directly calculated from the simulation and correspond to macroscopic observables.

The potential energy expressions used to drive molecular simulations can be broken down into individual components:

$$E_{\text{total}} = E_{\text{Coul}} + E_{\text{VDW}} + E_{\text{Bond}} + E_{\text{Angle}} + E_{\text{Torsion}} \quad (3.1)$$

where E_{Coul} and E_{VDW} represent non-bonded pairwise energies involving Coulomb (electrostatic) and short-range van der Waals interactions, respectively, between a pair of atoms. The remaining terms on the right-hand side of Eq. (3.1) refer to three- or four-body bonded interactions: bond stretch, angle bend, and dihedral torsion. Bonded interactions are necessary for polyatomic ions and molecules so that the molecular geometry remains consistent throughout a simulation. Some molecules with atoms in a planar arrangement (e.g. phenyl rings, carbonate ions) also require improper torsion energy terms to maintain this geometry.

A collection of energy expressions derived for a general type of model system is referred to as a ‘force field’. Force field parameters are derived by fitting the classical energy expressions to either experimental data or high-level quantum calculations. General force fields for organic molecules first began to appear in the 1980s and continue to see widespread use today. Examples include AMBER (Cornell et al., 1995), CVFF (Dauber-Osguthorpe et al., 1988), and OPLS (Jorgensen and Tiradorives, 1988). Force fields that rely solely on the energy expression given in Eq. (3.1) are referred to as Class 1 force fields. More complicated (and computationally costly) Class 2 force fields have been developed for use with complex biomolecules such as proteins and nucleic acids. In this case, additional energy terms are included that represent correlated motion between, for example, bond stretch and angle bend interactions. Generally, Class 1 force fields are sufficient for clay minerals and other oxide phases that have fairly rigid structures.

Several force fields specific to phyllosilicates were developed, including ClayFF (Cygan et al., 2004), PFF (Heinz et al., 2005), and several others (Skipper et al., 1991; Hill and Sauer, 1995; Teppen et al., 1997; Kawamura et al., 1999; Bougeard et al., 2000; Sato et al., 2001). Additional details on how these force fields were derived and their applications can be found in a recent review article (Cygan et al., 2009). This topic is further developed in Section 3.3.

3.3 FORCE FIELD DEVELOPMENT

Accuracy of the energy force field is of critical importance in the molecular simulation of clay mineral systems. Because of the lack of accurate interaction parameters, nearly all of the early simulations used constrained or rigid clay mineral structures. Most recent simulation studies incorporate force fields allowing full atomic flexibility. Full flexibility is especially important for analyzing local structure in the clay mineral interlayer space and for describing adsorption phenomena on external clay mineral surfaces. MD simulations, in particular, require atomic flexibility to ensure proper exchange of energy and momentum at interfaces between the clay mineral and aqueous solutions. There is practical evidence that, without this flexibility, determinations of dynamical properties such as diffusion of near-surface species and vibrational behaviour will be inaccurate.

Force field development specific to clay mineral applications typically involves parameterization of a chosen set of analytical expressions (Eq. 3.1) describing both non-bonded (Coulombic and van der Waals) interactions and bonded interactions between usually covalent components of the mineral. Practitioners of force field development have the choice of using (i) a covalent approach where bonded potentials (e.g. harmonic, Morse, etc.) describe the interaction energy of metal–oxygen interactions of the clay mineral layer, hydroxyl groups, and interlayer water molecules or (ii) an ionic approach where non-bonded potentials (e.g. Coulomb and Lennard–Jones) are used to reproduce the identical potential energy but with a combination of different potential energy functions. Furthermore, each force field approach relies on observed clay mineral and simple oxide refinements and spectroscopic data to derive the best fits and the necessary parameters for the interaction functions. Alternatively, force field parameterization can take advantage of quantum calculations (e.g. Hartree–Fock, density functional theory, etc.) where, perhaps, structural data are not available or where unusual or extreme conditions prevent determination of experimental data.

Many force fields for clay minerals use a bonded approach to describe the metal–oxygen interactions of the layer structure (e.g. [Teppen et al., 1997](#); [Kawamura et al., 1999](#); [Heinz et al., 2005](#)). Long-range electrostatic and short-range van der Waals interactions are evaluated for all atomic interactions of the system, but are excluded for any specific metal–oxygen bond. Interlayer water molecules are typically based on one of several traditional water models ([Jorgensen et al., 1983](#)) which can be held rigid or flexible with stretch and bend motions.

Alternatively, non-bonded force fields for clay mineral simulations such as ClayFF ([Cygan et al., 2004](#)) rely primarily on the electrostatic and van der Waals energy terms to describe the metal–oxygen bonding of the clay mineral layer structure. Water and hydroxyl groups are described by a flexible single point charge (SPC) water model ([Berendsen et al., 1981](#); [Teleman et al., 1987](#))

or a Morse potential (Greathouse et al., 2009). Partial charges on each atom, critical to non-bonded force fields, were determined using quantum chemical methods. Additionally, ClayFF considers the delocalization of charge at substitutional tetrahedral and octahedral sites and, therefore, provides a highly accurate description of clay mineral surface charge at the interlayer and external surfaces. Once partial charges are determined for each atom type, fitting of van der Waals parameters and other non-bonded terms is accomplished using an inverse modelling code such as GULP (Gale and Rohl, 2003) in which the observed structures of simple metal oxide compounds are used as input.

3.4 APPLICATIONS

Molecular simulations provide a previously unavailable opportunity to develop accurate models for the structure and dynamical behaviour of clay minerals. Building from the large volume of powder X-ray and neutron diffraction data and from recent X-ray absorption and X-ray reflectivity studies, molecular simulations studies offer a glimpse into possible models for the complex molecular behaviour of clay mineral systems. MD simulations, in particular, can capture the dynamical structure associated with cations and water molecules in the interlayer space and structural details of the clay mineral layers including site substitutions, vacancies, and hydroxyl behaviour.

3.4.1 Clay Mineral Swelling

An example of the swelling behaviour of Na^+ -Mt is provided by Cygan et al. (2004), where a series of MD simulations of a relatively small simulation cell (four unit cells) were used to model the expansion of the clay mineral layers due to increasing number of interlayer water molecules. Figure 3.3 displays the expansion of Na^+ -Mt by the change in basal *spacing* as a function of water content, derived from analysis of the MD trajectory of the equilibrated structures. The MD results closely map onto the experimental data and demonstrate the expansion of the clay mineral TOT layers with the insertion of water, reducing the Coulombic interactions while enhancing the relatively strong hydration of the interlayer Na^+ . The one-layer hydrate is stabilized at a basal spacing of approximately 12 Å, while continued insertion of water molecules leads to further cation hydration and the development of a strong hydrogen-bonded water network within the interlayer. Ultimately, further addition of water molecules expands the Mt, leading to the formation of a stable two-layer hydrate. The simulations suggest a slight stabilization of a three-layer hydrate, but for the Wyoming Mt composition the layer structures continue to expand with higher water contents, at least in the virtual world. Several simulation studies (e.g. Boek, 1995; Kawamura et al., 1999; Smith et al., 2006; Zheng et al., 2011) successfully modelled the swelling of smectites under a variety of conditions and water content.

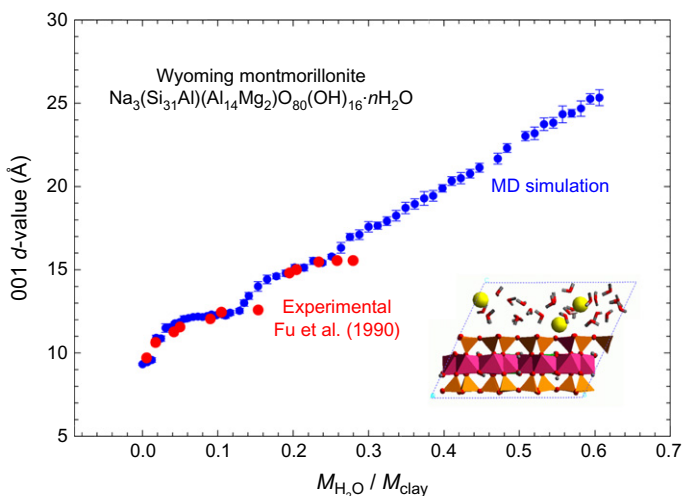


FIGURE 3.3 Swelling behaviour of Na^+ -Mt obtained from a series of *NPT* MD simulations. The modelling results, showing the sequential expansion of the Mt with water content, are in agreement with the experimental data of Fu et al. (1990).

3.4.2 Interlayer Structure and Dynamics

The computer storage of atomic positions and velocities for time steps associated with MD simulation, referred to as a ‘trajectory’, provides a convenient method for analysis of the clay mineral structure. For example, the layer and interlayer structure of Na^+ -Mt can be determined by sampling the atomic positions stored in the trajectory file once the structure has equilibrated. Figure 3.4 provides the relative atomic density profiles of all Na^+ -Mt atoms across the clay mineral layer for an equilibrated two-layer hydrate. The layered clay mineral structure is clearly identified by the dominant peaks for the atoms of the silicate tetrahedra and alumina octahedra, and by smaller peaks for the octahedral Mg and tetrahedral Al substitutions. Hydroxyl groups defined by O_H and H_C typically occur parallel to the layers, although there is evidence that some of the hydroxyl groups are oriented normal to the layers towards the tetrahedral Al site. The relatively diffuse behaviour of water in the interlayer region is represented by two broad O peaks and by five broad overlapping H peaks. Hydrogen atoms are oriented towards either side of the O peaks and suggest a water dipole oriented in response to the negatively charged clay mineral layer. Interlayer Na^+ occurs primarily in the central region of the interlayer space fully coordinated by water, although the profile exhibits some Na^+ density near the tetrahedral layer having Al substitution (inner sphere complex).

Figure 3.5 highlights the atomic density profiles for virtual hydrated pyrophyllite, two Na^+ -Mt (one with pure octahedral charge and one with slight

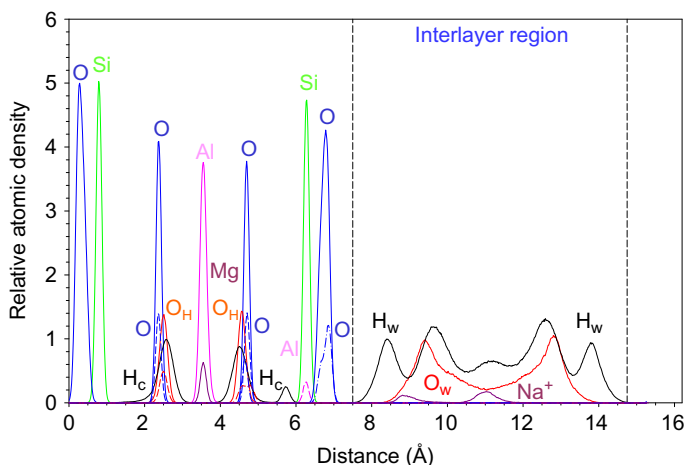


FIGURE 3.4 Atomic density profiles of a two-layer hydrate of Na^+ -Mt derived from the 100-ps trajectory of an equilibrated MD simulation.

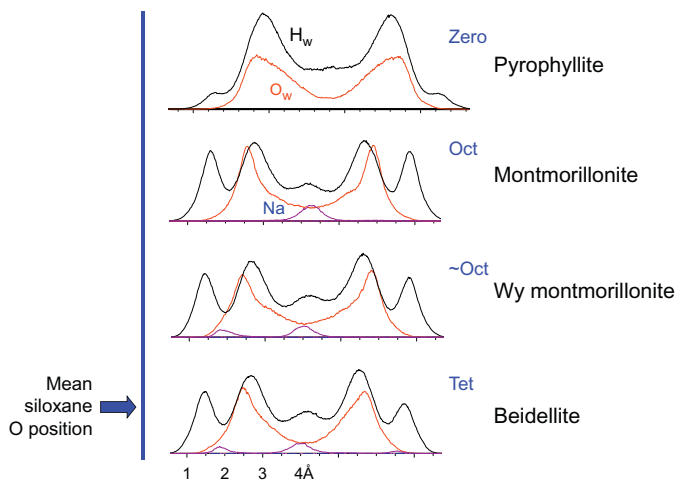


FIGURE 3.5 Atomic density profiles for the interlayer atoms obtained from the trajectories of equilibrated MD simulations of a hydrated pyrophyllite (virtual phase) and three smectites. The mean position of the silicate O surface and the sheet location of layer charge are indicated.

additional tetrahedral charge, i.e. Wyoming Mt and Na^+ -beidellite (Bd). Pyrophyllite displays a unique water distribution in the interlayer space, suggesting a relatively hydrophobic environment with limited interaction of the hydrogen atom of water with the clay mineral layer. The three smectites exhibit similar profiles with slight modifications in response to the Na^+ and the location of

the layer charge. Additionally, the MD results clearly show a variation in the basal spacing due to the type and location of the layer charge. Atomic density profiles for other crystallographic directions and atomic density maps for specific planes and interfaces can be similarly derived from the MD trajectories. Ultimately, the atomic densities can be compared with experimental X-ray absorption and X-ray reflectivity methods (Brown and Sturchio, 2002; Fenter and Sturchio, 2004).

In contrast to MC simulations, MD methods provide a deterministic approach for examining the evolution of a molecular system, providing insights into diffusion processes and other dynamical behaviour. Diffusion rates of water and cations in the interlayer space of clay minerals can be determined by analysis of atomic trajectories and plotting the mean square displacement (MSD) of species as a function of simulation time. Results from a MD simulation of Na^+ -Mt using an NPT ensemble are presented in Fig. 3.6, where, after one million time steps of simulation, significant water and Na^+ diffusion occurs. Diffusion rates are derived from the slope of the MSD versus time plot

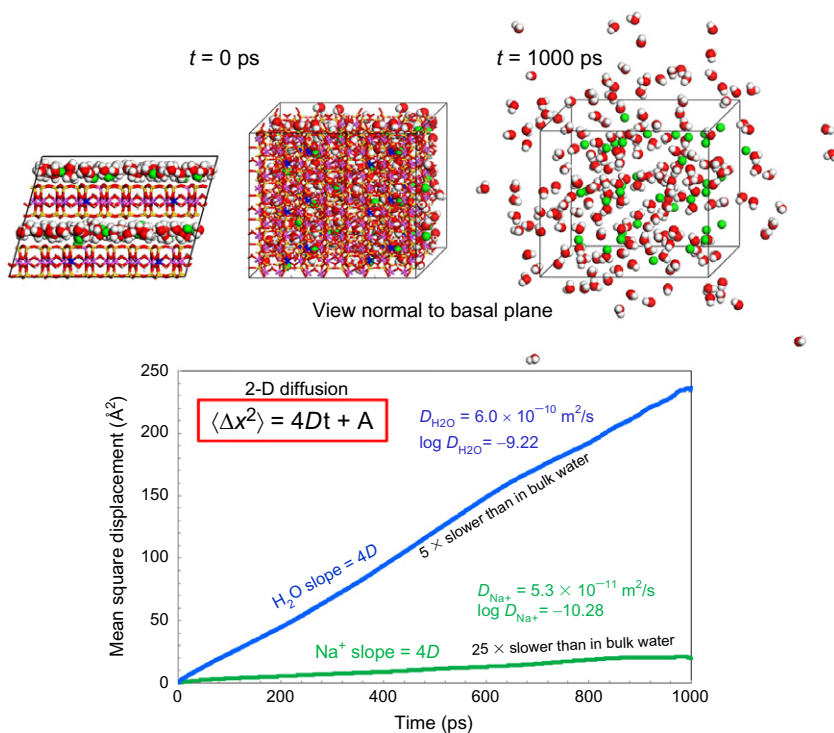


FIGURE 3.6 Snapshots from MD simulation of Na^+ -Mt; the far right model displays only interlayer species and relative extent of water and Na^+ diffusion. Diffusion rates are obtained from slope of mean square displacement for water oxygens and Na^+ as function of time.

based on the Einstein relation for diffusion in a planar geometry characteristic of the interlayer space of clay minerals (Frenkel and Smit, 2002). Water diffusion within the interlayer of Na^+ -Mt is about 5 times slower than in bulk water, while Na^+ diffusion in the interlayer is 25 times slower; diffusion rates for water in Mt are 10 times faster than Na^+ . These MD results are consistent with recent neutron scattering experiments completed by Malikova et al. (2010). Similar modelling approaches have recently been used to evaluate the diffusion of cations and water in the interlayer space and on the external surfaces of clay minerals (Rotenberg et al., 2007; Bourg and Sposito, 2010, 2011; Churakov and Gimmi, 2011).

Molecular simulation also provides a rigorous path towards modelling and interpreting results from X-ray diffraction analysis, molecular spectroscopies, and other analytical methods. In particular clay minerals, because of stacking disorder and difficulties in crystallographic refinements, can be systematically evaluated by molecular simulation to evaluate structure and molecular behaviour. Given a molecular model of a clay mineral structure, an X-ray diffraction pattern can be calculated and directly compared with experimental diffraction patterns. Basal spacing for ordered and mixed-layer stacking sequences can be systematically determined, or the expansion of clay minerals with varying water content or other intercalate compounds can be derived (see Fig. 3.3).

Vibrational behaviour and other related spectroscopic processes associated with clay minerals were studied by MD simulation. For example, Ockwig et al. (2009) obtained inelastic neutron scattering data on the vibrational behaviour of water in fibrous clay minerals such as sepiolite and palygorskite, which indicated a significant shift in the band of librational modes (i.e. rock, wag, and twist motions) between the two differently sized water channels. Analysis of the trajectories from large-scale MD simulations of the two minerals used power spectra obtained from the velocity autocorrelation function (Frenkel and Smit, 2002). Correlations of atomic velocities suggest coordinated motions of interacting atoms (i.e. molecular vibrations) in the simulation cell and can be used to quantify bond stretch, bond bend, libration, and complex hydrogen-bond motions (Fig. 3.7). In the fibrous mineral study, the experimental and simulated librational band for water in sepiolite was shifted to higher frequencies and was interpreted to be the result of increased hydrogen bonding of water molecules at the inversion of the tetrahedral sheet, which were less favoured by the smaller and distorted channels in palygorskite.

3.4.3 Solute Adsorption

Recently, MD simulations were used to investigate the adsorption of aqueous species onto clay mineral surfaces. Such simulations require a large simulation cell to adequately model a bulk aqueous solution in contact with the clay mineral surface. Schematics of two such simulation cells are shown in

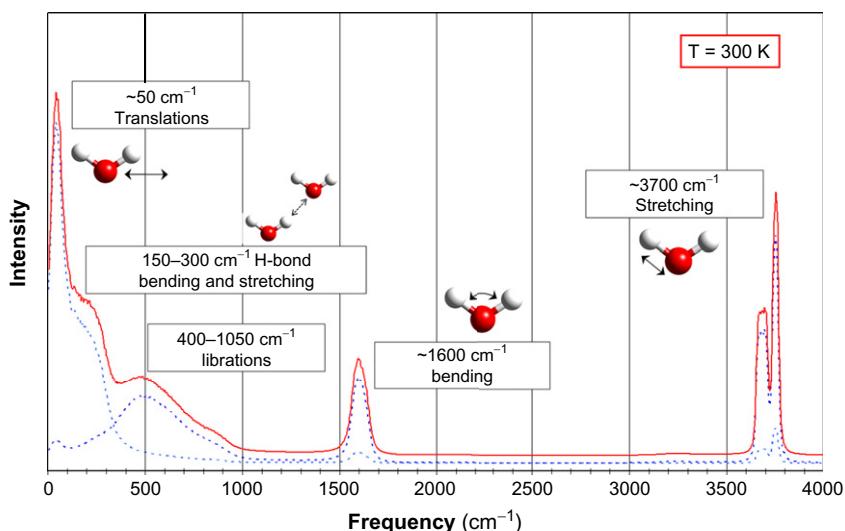


FIGURE 3.7 Power spectra of water derived from atomic trajectory obtained from equilibrated MD simulation of bulk water; red line represents the total spectrum, and blue lines represent the spectra for hydrogen and oxygen atoms.

Fig. 3.8. The mineral phase must be sufficiently thick so that species in the solution phase have no short-range interactions beyond the surface layers. Also, care must be taken so that any net charge in the clay mineral layers is balanced by the opposite charge in the aqueous phase. After defining the adsorbed and diffuse layers in the simulation cell (**Fig. 3.9**), the adsorption of aqueous species onto the clay mineral surface is quantified using atomic density profiles.

MD simulations were used to study the adsorption of aqueous uranyl (UO_2^{2+}) ions onto clay mineral surfaces in the presence of carbonate ions in aqueous solutions (**Greathouse and Cygan, 2005, 2006**). Electroneutrality constraints required that the aqueous region contain cations (Na^+) to balance the negative charge of the external clay mineral surface, and that each uranyl ion in the aqueous phase be accompanied by an anion. In this case, carbonate was used, and pH effects were simulated by adjusting the $\text{UO}_2\text{CO}_3(\text{aq})$ concentration. The adsorption and desorption of the ions onto the Mt surface could be treated as an equilibrium process, from which trends in equilibrium partition coefficients (K_D) were observed. Uranyl adsorption decreases as the concentration of uranyl (and carbonate) ions in the aqueous phase increases (**Fig. 3.10**). The concentration of the sodium ions in solution remains fixed throughout these simulations, and sodium adsorption is unaffected by changes in uranyl carbonate concentrations. The difference in adsorption behaviour between sodium and uranyl ions is explained by the ability of the latter to

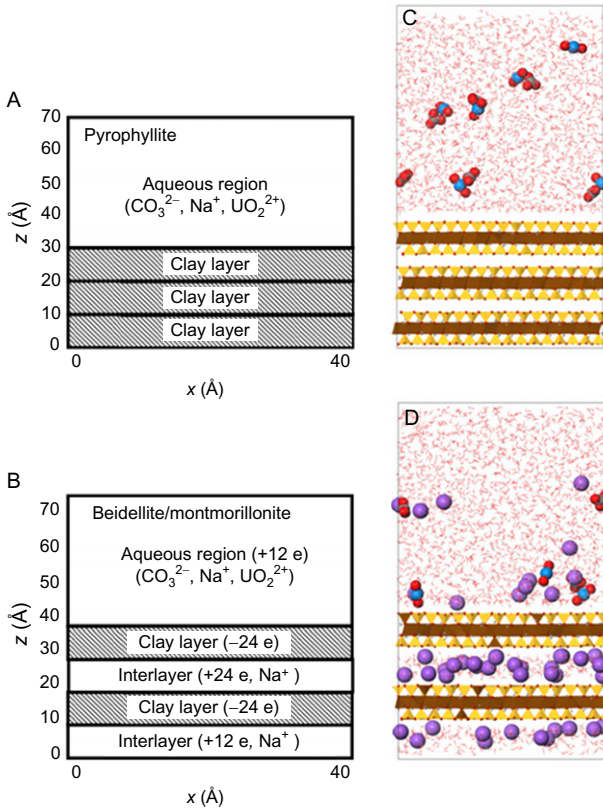


FIGURE 3.8 Schematic of MD simulation cells containing external clay mineral surfaces in contact with an aqueous solution (Greathouse and Cygan, 2006). A pyrophyllite surface is shown in (A) and (C). A smectite surface is shown in (B) and (D). Copyright 2006, American Chemical Society.

form aqueous complexes with carbonate ions. These complexes can be charge-neutral or anionic, thus reducing their electrostatic attraction to the Mt surface. The trend in uranyl adsorption is confirmed by batch adsorption experiments, which show drastically reduced uranyl adsorption onto Mt above pH 9 (Pabalan et al., 1998).

By comparing uranyl adsorption onto Mt with a neutral clay mineral (pyrophyllite) and a smectite with exclusively tetrahedral charge (Bd), Greathouse and Cygan (2006) were able to further investigate adsorption trends. By quantifying the abundance and speciation of uranyl complexes in the aqueous phase near these surfaces (Fig. 3.11), several trends became evident. The abundance of the neutral $\text{UO}_2\text{CO}_3(\text{aq})$ complex increased with increasing uranyl (and carbonate) concentration. At higher concentrations, $[\text{UO}_2(\text{CO}_3)_2]^{2-}$ and oligomeric species were also seen in the aqueous phase. For the smectites, the location of negative charge within the mineral lattice (octahedral sheet for Mt, tetrahedral sheet for Bd) had little effect on

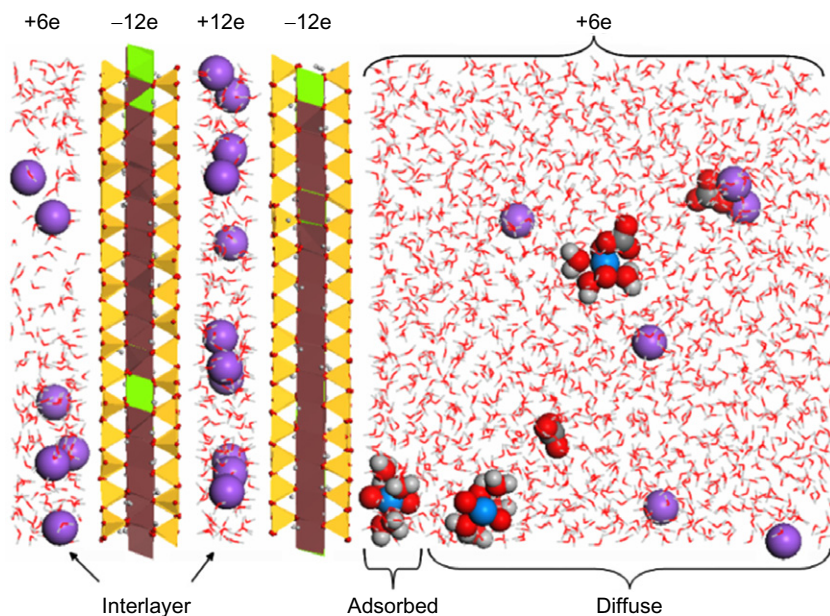


FIGURE 3.9 Equilibrium snapshot from an adsorption simulation consisting of $\text{UO}_2\text{CO}_3(\text{aq})$ and charge-balancing $\text{Na}^+(\text{aq})$ near an external Mt surface (Greathouse and Cygan, 2005). Labels at the top indicate the net electrostatic charge for each aqueous and clay mineral phase. Reproduced by permission of PCCP Owner Societies.

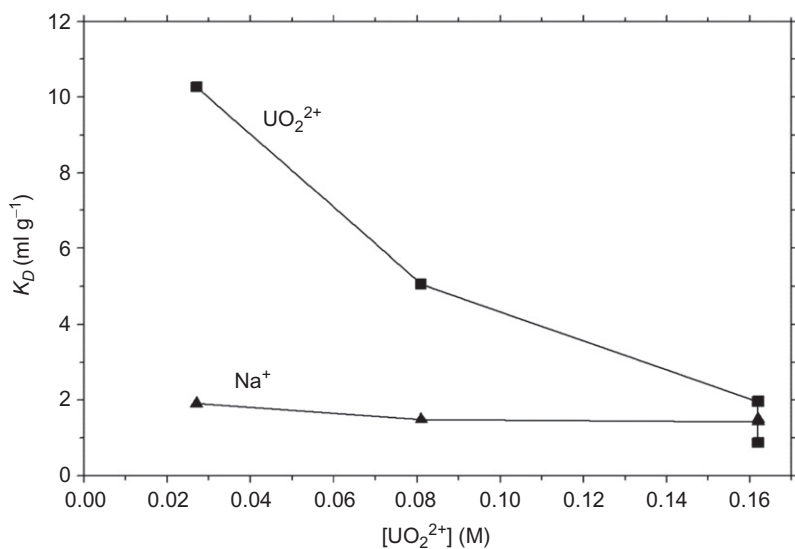


FIGURE 3.10 Equilibrium partition coefficients (K_D) for Na^+ and UO_2^{2+} adsorption onto an external Mt surface (Greathouse and Cygan, 2005). Reproduced by permission of the PCCP Owner Societies.

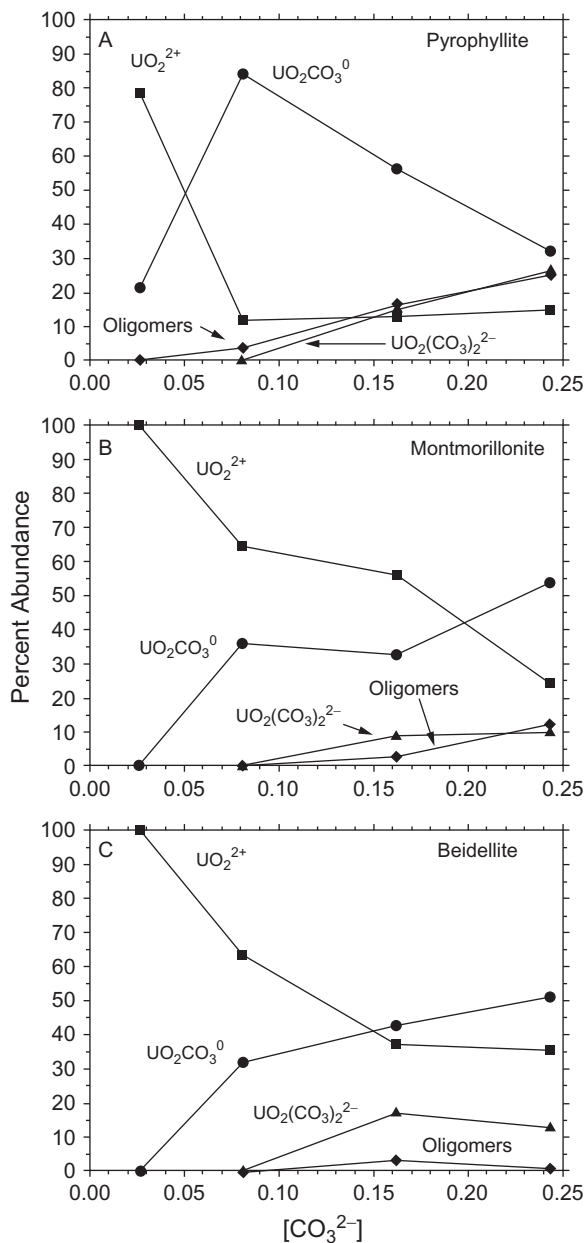


FIGURE 3.11 Uranyl speciation in the diffuse aqueous regions near (A) pyrophyllite, (B) Mt, and (C) Bd surfaces (Greathouse and Cygan, 2006). Copyright 2006, American Chemical Society.

uranyl speciation. The neutral pyrophyllite surface resulted in much higher abundances of uranyl carbonate complexes throughout the range of solution composition.

Similar methods were used to investigate the formation of electrical double layers near external smectite surfaces (Tournassat et al., 2009; Bourg and Sposito, 2011). Na^+ and Cl^- profiles near the surface were used to constrain the corresponding electrical double-layer parameters in the triple-layer model (Tournassat et al., 2009). Simulations of a mixed NaCl – CaCl_2 electrolyte near the surface resulted in redefined ion adsorption planes often used in double-layer models (Bourg and Sposito, 2011). MD simulations were also used to study the structure and dynamics of water near an external muscovite surface (Wang et al., 2005; Sakuma and Kawamura, 2009). The charge-balancing K^+ ions remained adsorbed at the external surface despite the presence of a thick (3–10 nm) water layer. Adsorbed water was found to be highly ordered, influencing water structure several molecular diameters from the surface. Finally, Vasconcelos et al. (2007) used MD simulation to investigate the equilibrium partitioning of aqueous cations and anions at the basal surfaces of an expanded kaolinite pore. Interestingly, the anion (Cl^-) preferentially adsorbed to the hydroxylated alumina surface via inner-sphere complexation, while the cations (Na^+ , Cs^+ , Cd^{2+} , Pb^{2+}) adsorbed to the siloxane surface; only Cs^+ showed a strong tendency for inner-sphere adsorption.

3.5 CONCLUDING REMARKS

Much of the recent development in molecular simulations of clay minerals is associated with the use of massively parallel supercomputers to examine increasingly larger and more complex simulation cells. MD simulations of clay mineral systems having millions of atoms are not that uncommon and have led to improved understanding of the mechanical properties of clay minerals (Suter et al., 2007; Suter and Coveney, 2009) and the intercalation of biomolecules (Thyveetil et al., 2008; Swadling et al., 2010). In addition, with more powerful computer systems, quantum mechanical tools, primarily density functional methods, have provided efficient algorithms for simulating the dynamical behaviour of clay minerals. Rather than relying on an empirical force field used in classical MD, *ab initio* molecular dynamics (AIMD) methods iteratively solve the Schrödinger equation for the potential energy (approximate solution) at each dynamic time step of the simulation. Of course, computational cost is extreme, and AIMD simulation cells are necessarily quite small in comparison to those typically used in traditional classical MD simulations. Nonetheless, the state of the art represented by AIMD methods will continue to lead to new developments in computational clay mineralogy, especially with ongoing advances in software and computer platforms.

Another growing area is the simulation of hybrid organic–inorganic materials. Organically modified clay minerals (organoclays) are prepared by substituting

the inorganic exchangeable cations of a natural or synthetic clay mineral with organic cations such as alkylammonium ions (smectites) or alkylsulphate ions (LDH). The basal spacing is greatly increased after such a substitution, and the resulting clay mineral surface is organophilic. Examples of the application of organoclays to industrial problems include drilling fluids (Anderson et al., 2010), water treatment (Beall, 2003), and clay mineral–polymer nanocomposites (Chen et al., 2008). Much of the simulation effort to date has focused on the structural, mechanical, and thermodynamic properties of organoclays (Greenwell et al., 2006; Cygan et al., 2009). Scocchi et al. (2007) used results from atomistic MD simulations of organoclays as input parameters for mesoscale simulations of clay mineral–polymer nanocomposites. Finally, simulations were also applied to the interaction of biomolecules with layered double hydroxide surfaces (Anderson et al., 2009). Most published simulation studies of organoclays have used an *ad hoc* approach for inorganic–organic interaction parameters. A combined force field that accurately describes both organic compounds and inorganic compounds and materials (and their interfaces) continues to be an area of active research.

It is appropriate to emphasize that molecular simulations of clay minerals provide a unique view of the clay mineral structures and offer molecular insights on the mechanisms of clay mineral interlayer and surface processes. Simulation methods have rapidly evolved over the last few decades and have matured to offer clay scientists an exceptional opportunity to test conceptual models and hypotheses regarding clay minerals and their behaviour. Molecular modelling provides a new and important tool to supplement the conventional analytical methods used to question nature's original nanomaterial.

REFERENCES

- Anderson, R.L., Greenwell, H.C., Suter, J.L., Coveney, P.V., Thyveetil, M.A., 2009. Determining materials properties of natural composites using molecular simulation. *J. Mater. Chem.* 19, 7251–7262.
- Anderson, R.L., Ratcliffe, I., Greenwell, H.C., Williams, P.A., Cliffe, S., Coveney, P.V., 2010. Clay swelling—a challenge in the oilfield. *Earth-Sci. Rev.* 98, 201–216.
- Beall, G.W., 2003. The use of organo-clays in water treatment. *Appl. Clay Sci.* 24, 11–20.
- Berendsen, H.J.C., Postma, J.P.M., von Gunsteren, W.F., Hermans, J., 1981. Interaction models for water in relation to protein hydration. In: Pullman, B. (Ed.), *Intermolecular Forces*. Reidel, Dordrecht, pp. 331–342.
- Boek, E.S., 1995. Molecular modeling of clay hydration: a study of hysteresis loops in the swelling curves of sodium montmorillonite. *Langmuir* 11, 4629–4631.
- Bougeard, D., Smirnov, K.S., Geidel, E., 2000. Vibrational spectra and structure of kaolinite: a computer simulation study. *J. Phys. Chem. B* 104, 9210–9217.
- Bourg, I.C., Sposito, G., 2010. Connecting the molecular scale to the continuum scale for diffusion processes in smectite-rich porous media. *Environ. Sci. Technol.* 44, 2085–2091.
- Bourg, I.C., Sposito, G., 2011. Molecular dynamics simulations of the electrical double layer on smectite surfaces contacting concentrated mixed electrolyte (NaCl–CaCl₂) solutions. *J. Colloid Interface Sci.* 360, 701–715.

- Brown, G.E., Sturchio, N.C., 2002. An overview of synchrotron radiation applications to low temperature geochemistry and environmental science. In: Fenter, P.A., Rivers, M.L., Sturchio, N.C., Sutton, S.R. (Eds.), *Applications of Synchrotron Radiation in Low-Temperature Geochemistry and Environmental Sciences. Reviews in Mineralogy and Geochemistry*, vol. 49. Mineralogical Society of America, Washington, DC, pp. 1–115.
- Chen, B., Evans, J.R.G., Greenwell, H.C., Boulet, P., Coveney, P.V., Bowden, A.A., Whiting, A., 2008. A critical appraisal of polymer-clay nanocomposites. *Chem. Soc. Rev.* 37, 568–594.
- Churakov, S.V., Gimmi, T., 2011. Up-scaling of molecular diffusion coefficients in clays: a two-step approach. *J. Phys. Chem. C* 115, 6703–6714.
- Cornell, W.D., Cieplak, P., Bayly, C.I., Gould, I.R., Merz, K.M., Ferguson, D.M., Spellmeyer, D.C., Fox, T., Caldwell, J.W., Kollman, P.A., 1995. A second generation force field for the simulation of proteins, nucleic acids, and organic molecules. *J. Am. Chem. Soc.* 117, 5179–5197.
- Cygan, R.T., 2001. Molecular modeling in mineralogy and geochemistry. In: Cygan, R.T., Kubicki, J.D. (Eds.), *Molecular Modeling Theory: Applications in the Geosciences. Reviews in Mineralogy and Geochemistry*, vol. 42. Mineralogical Society of America, Washington, DC, pp. 1–35.
- Cygan, R.T., Liang, J.-J., Kalinichev, A.G., 2004. Molecular models of hydroxide, oxyhydroxide, and clay phases and the development of a general force field. *J. Phys. Chem. B* 108, 1255–1266.
- Cygan, R.T., Greathouse, J.A., Heinz, H., Kalinichev, A.G., 2009. Molecular models and simulations of layered minerals. *J. Mater. Chem.* 19, 2470–2481.
- Dauber-Osguthorpe, P., Roberts, V.A., Osguthorpe, D.J., Wolff, J., Genest, M., Hagler, A.T., 1988. Structure and energetics of ligand binding to proteins: Escherichia coli dihydrofolate reductase-trimethoprim, a drug-receptor system. *Proteins: Struct. Funct. Genet.* 4, 31–47.
- Delville, A., 1991. Modeling the clay-water interface. *Langmuir* 7, 547–555.
- Fenter, P., Sturchio, N.C., 2004. Mineral-water interfacial structures revealed by synchrotron X-ray scattering. *Prog. Surf. Sci.* 77, 171–258.
- Frenkel, D., Smit, B., 2002. *Understanding Molecular Simulation: From Algorithms to Applications*. Academic Press, San Diego.
- Fu, M.H., Zhang, Z.Z., Low, P.F., 1990. Changes in the properties of a montmorillonite-water system during the adsorption and desorption of water: hysteresis. *Clays Clay Miner.* 38, 485–492.
- Gale, J.D., Rohl, A.L., 2003. The general utility lattice program (GULP). *Mol. Simulat.* 29, 291–341.
- Greathouse, J.A., Cygan, R.T., 2005. Molecular dynamics simulation of uranyl(VI) adsorption equilibria onto an external montmorillonite surface. *Phys. Chem. Chem. Phys.* 7, 3580–3586.
- Greathouse, J.A., Cygan, R.T., 2006. Water structure and aqueous uranyl(VI) adsorption equilibria onto external surfaces of beidellite, montmorillonite, and pyrophyllite: results from molecular simulations. *Environ. Sci. Technol.* 40, 3865–3871.
- Greathouse, J.A., Durkin, J.S., Larentzos, J.P., Cygan, R.T., 2009. Implementation of a Morse potential to model hydroxyl behavior in phyllosilicates. *J. Chem. Phys.* 130, 134713.
- Greenwell, H.C., Jones, W., Coveney, P.V., Stackhouse, S., 2006. On the application of computer simulation techniques to anionic and cationic clays: a materials chemistry perspective. *J. Mater. Chem.* 16, 708–723.
- Heinz, H., Koerner, H., Anderson, K.L., Vaia, R.A., Farmer, B.L., 2005. Force field for mica-type silicates and dynamics of octadecylammonium chains grafted to montmorillonite. *Chem. Mater.* 17, 5658–5669.

- Hill, J.-R., Sauer, J., 1995. Molecular mechanics potential for silica and zeolite catalysts based on *ab initio* calculations. 2. Aluminosilicates. *J. Phys. Chem.* 99, 9536–9550.
- Jorgensen, W.L., Tiradorives, J., 1988. The OPLS potential functions for proteins. Energy minimizations for crystals of cyclic peptides and crambin. *J. Am. Chem. Soc.* 110, 1657–1666.
- Jorgensen, W.L., Chandrasekhar, J., Madura, J.D., Impey, R.W., Klein, M.L., 1983. Comparison of simple potential functions for simulating liquid water. *J. Chem. Phys.* 79, 926–935.
- Kawamura, K., Ichikawa, Y., Nakano, M., Kitayama, K., Kawamura, H., 1999. Swelling properties of smectite up to 90 degrees C: in situ X-ray diffraction experiments and molecular dynamic simulations. *Eng. Geol.* 54, 75–79.
- Malikova, N., Dubois, E., Marry, V., Rotenberg, B., Turq, P., 2010. Dynamics in clays—combining neutron scattering and microscopic simulation. *Z. Phys. Chem.* 224, 153–181.
- Ockwig, N.W., Greathouse, J.A., Durkin, J.S., Cygan, R.T., Daemen, L.L., Nenoff, T.M., 2009. Nanoconfined water in magnesium-rich 2:1 phyllosilicates. *J. Am. Chem. Soc.* 131, 8155–8162.
- Pabalan, R.T., Turner, D.R., Bertetti, F.P., Prikryl, J.D., 1998. Uranium(VI) sorption onto selected mineral surfaces. In: Jenne, E. (Ed.), *Adsorption of Metals by Geomedia: Variables, Mechanisms, and Model Applications*. Academic Press, San Diego, pp. 99–130.
- Rotenberg, B., Marry, V., Vuilleumier, R., Malikova, N., Simon, C., Turq, P., 2007. Water and ions in clays: unraveling the interlayer/micropore exchange using molecular dynamics. *Geochim. Cosmochim. Acta* 71, 5089–5101.
- Sakuma, H., Kawamura, K., 2009. Structure and dynamics of water on muscovite mica surfaces. *Geochim. Cosmochim. Acta* 73, 4100–4110.
- Sato, H., Yamagishi, A., Kawamura, K., 2001. Molecular simulation for flexibility of a single clay layer. *J. Phys. Chem. B* 105, 7990–7997.
- Scocchi, G., Posocco, P., Danani, A., Pricl, S., Fermeglia, M., 2007. To the nanoscale, and beyond! Multiscale molecular modeling of polymer-clay nanocomposites. *Fluid Phase Equilib.* 261, 366–374.
- Skipper, N.T., Refson, K., McConnell, J.D.C., 1991. Computer simulation of interlayer water in 2:1 clays. *J. Chem. Phys.* 94, 7434–7445.
- Smith, D.E., Wang, Y., Chaturvedi, A., Whitley, H.D., 2006. Molecular simulations of the pressure, temperature, and chemical potential dependencies of clay swelling. *J. Phys. Chem. B* 110, 20046–20054.
- Suter, J.L., Coveney, P.V., 2009. Materials properties of clay nanocomposites: onset of negative Poisson ratio in large-scale molecular dynamics simulation. *Soft Matter.* 5, 3896–3904.
- Suter, J.L., Coveney, P.V., Greenwell, H.C., Thyveetil, M.A., 2007. Large-scale molecular dynamics study of montmorillonite clay: emergence of undulatory fluctuations and determination of material properties. *J. Phys. Chem. C* 111, 8248–8259.
- Swadling, J.B., Coveney, P.V., Greenwell, H.C., 2010. Clay minerals mediate folding and regioselective interactions of RNA: a large-scale atomistic simulation study. *J. Am. Chem. Soc.* 132, 13750–13764.
- Teleman, O., Jonsson, B., Engstrom, S., 1987. A molecular dynamics simulation of a water model with intramolecular degrees of freedom. *Mol. Phys.* 60, 193–203.
- Teppen, B.J., Rasmussen, K.R., Bertsch, P.M., Miller, D.M., Schafer, L., 1997. Molecular dynamics modeling of clay minerals. 1. Gibbsite, kaolinite, pyrophyllite, and beidellite. *J. Phys. Chem. B* 101, 1579–1587.
- Thyveetil, M.A., Coveney, P.V., Greenwell, H.C., Suter, J.L., 2008. Computer simulation study of the structural stability and materials properties of DNA-intercalated layered double hydroxides. *J. Am. Chem. Soc.* 130, 4742–4756.

- Tournassat, C., Chapron, Y., Leroy, P., Bizi, M., Boulahya, F., 2009. Comparison of molecular dynamics simulations with triple layer and modified Gouy-Chapman models in a 0.1 M NaCl-montmorillonite system. *J. Colloid Interface Sci.* 339, 533–541.
- Vasconcelos, I.F., Bunker, B.A., Cygan, R.T., 2007. Molecular dynamics modeling of ion adsorption to the basal surfaces of kaolinite. *J. Phys. Chem. C* 111, 6753–6762.
- Wang, J.W., Kalinichev, A.G., Kirkpatrick, R.J., Cygan, R.T., 2005. Structure, energetics, and dynamics of water adsorbed on the muscovite (001) surface: a molecular dynamics simulation. *J. Phys. Chem. B* 109, 15893.
- Zheng, Y., Zaoui, A., Shahrou, I., 2011. A theoretical study of swelling and shrinking of hydrated Wyoming montmorillonite. *Appl. Clay Sci.* 51, 177–181.